NANOPARTICLE-AEROSOL TECHNOLOGY: A NOVEL APPROACH FOR THE DEVELOPMENT OF METAL ALLOYS

A Thesis

Presented to the Faculty of the Graduate School

of Cornell University

In Partial Fulfillment of the Requirements for the Degree of

Master of Science

by

Rui Yang

December 2017

ABSTRACT

A series of new steel alloys were prepared by injecting particle aerosols into molten steel using an experimental set up (bench top furnace equipped with an aerosolizer) designed, built, and commissioned at Cornell. The introduction of the various particles, especially nanoparticles, results in significantly altered microstructure (grain size and morphology). The target metal particles or mixtures of particles are aerosolized first and carried into the molten metal for alloying. Cast iron and 1018 steel are chosen as the raw materials while metal powders (Ti, W, Nb) with different size scale (micron and nano-scale) are alloyed into the molten metals through different approaches (regular alloying and aerosol technology). Compared to the alloys produced by conventional metallurgy (regular alloying and regular size particles), the new alloys exhibit significantly altered microstructures and refinement of grain size, and much better uniform distribution as observed with EDS element mapping. The experiments confirm that the nanoparticle-aerosol technology is a promising approach with good versatility and can realize excellent dispersion of alloyed agents even with trace amount of injection. Moreover, this approach is shown to be more advantageous over conventional metallurgy and seems to have potential in industrial applications.

BIOGRAPHICAL SKETCH

Rui Yang was born and raised in China, in the city of Zhongshan and grew up in Shenzhen. He was the only child. When he was in high school, he became fascinated by the concept “entropy” during his studies in thermodynamics. He was so astonished about its wide implication, especially when he used this theory to verify real-world phenomena. From then on, he has been immersing himself in the mystery of chemistry, holding the belief that the experimental observations will enable him to have a better understanding of the intrinsic rules of the world.

Then he was admitted to Sun Yat-sen University, one of the top 10 universities in China, at the age of 18. As a student in the School of Chemistry and Chemical Engineering he majored in Polymeric Materials and Engineering. Yang was equipped with a solid foundation of theoretical knowledge and experimental skills. In July 2014, he gained his first internship in Amcor Flexibles Foshan DQ Co., LTD., which was mainly to investigate the possibility of improving the performance of multifunctional plastic films through continuous biaxial drawing technology. This experience was the first time that he realized how important having a sound theoretical basis was, because only with sufficient basic knowledge can one identify the key factors and have the idea to improve a product. Moreover, he also found that doing research is much more complicated than merely understanding concepts in textbooks — but also much more rewarding. Yang was also very interested in research topics about application of materials and worked with Professor Kancheng Mai in the study of Preparation of Antibacterial PPR Composites as his graduation project.

After graduation from Sun Yat-sen University, Yang continued his master candidate life at Cornell University and focused on graduate studies of materials science. At Cornell, Yang joined Professor Emmanuel P. Giannelis's research group. During his two-year master's program, Dr Wenyang Pan in this group gave him a lot of help. They worked together on the same project and solved many difficulties they met. Also, he was greatly inspired by his advisor that encouraged his scientific curiosity. His work at Cornell was focused on developing novel Nanoparticle-Aerosol Technology for the development of metal alloys.

Now, Yang is still working on the same project for metal alloys and participating in other projects at the same time at Cornell. For his future, he plans to continue his studies in a PhD program on the development of novel materials and their applications.

Dedicated to all the people who have helped me at Cornell and to my parents: for always encouraging me, supporting me, and trusting me.

ACKNOWLEDGMENTS

First, I want to express my deepest gratitude to my parents, Jianwen Yang and Zaichun Hu, for their love, patience, trust and their great support in my life. Their kindness, intelligence and humility have always inspired me to be a better person.

I would also like to acknowledge my advisor, Emmanuel, who gave me his expert advice, support and encouragement during my two-year study at Cornell. I was so lucky to get the chance to work and learn under his guidance. I have not just learned how to do research but also the way to collaborate and communicate with others. I truly appreciate it.

To my committee member, Professor Robert Shepherd, thank you for serving in my committee.

To my collaborator in the research work presented in this thesis, Pan, really thank you for always being with me to face and fight those uncertainties, difficulties and failures we met during the 2-year project. Without your help and advice, it would be impossible for me alone to establish the frame and foundation of this project from nothing, let alone the breakthroughs we gained. Thank you for your friendship and patience, you are more like my family instead of a postdoc who guided my research. I really appreciate that I was admitted to Cornell and have the chance to meet you and Prof. Emmanuel. The two years life in our group is truly an unforgettable experience in my life.

To all group members, you are all incredibly skillful people and it was very pleasant to work with you all.

TABLE OF CONTENTS

LIST OF FIGURES

LIST OF TABLES

CHAPTER 1

1. Introduction

1.1 Metal Alloys

Metal alloys are materials, which are made up of at least two different chemical elements, one of which is a metal. With the addition of other elements, the metal alloys can exhibit better properties including better strength, hardness and corrosion resistance compared to the parent metal. Nowadays, our daily life has been firmly connected with products based on metal alloys. In addition to those widely used alloy products like kitchen utensils which are made of cast iron (high carbon content iron alloy), others include the light alloy wheel in automotive industry or the high strength steel for construction purposes [1-4]. Nevertheless, with the development of science and technology, demands for super high performance alloy also arise. For instance, electrical engineering demands novel alloys with both superior mechanical strength and good electrical conductivity to be used as the wire for power transmission line[5]. Nuclear energy industry is also looking for affordable metal alloys which can maintain mechanical properties at elevated temperature, to avoid using those expensive high melting point pure metals as the materials to build nuclear fission reactors [6].

1.2 Nanotechnology

Many efforts have been made to the development of super high performance alloys, one of which is applying nanotechnology. Nanotechnology aims at developing novel

materials with revolutionary physical, chemical, mechanical or optical properties by controlling or modifying materials at the molecular or nanometer scale. Nanomaterials, such as nanoparticles (NPs), exhibit properties different from their micro/macro-scale counterparts especially when they serve as the fillers to prepare composites. Efforts have included introducing nanoparticles into the metal matrix during the preparation to realize nanostructural design and control, and achieve improved properties without tradeoffs. One successful example was Sandvik Nanoflex, a class of steel alloys with ultra-high strength, great formability and corrosion resistance. Those superior properties were achieved by introducing nanoscale precipitates/clusters into steel during processing. The improved properties results from the precipitation of extremely hard, nanoscale particles formed in a semi-hard state during the heat treatment. The favorable nucleation conditions assist to disperse uniformly the clusters in the steel. Compared with regular steel, Sandvik Nanoflex exhibits as much as 80% improvement in tensile strength without compromising ductility [7,8]. This kind of alloy is called microalloyed steels, also known as the high strength low-alloy (HSLA) steels, which exhibit a combination of high strength, toughness, resistance to corrosion and good weldability by adding very low amounts of certain elements (Ti, Nb or V) to low carbon steels (0.05-0.25%) [9,10]. The improved properties in HSLA steels result from the grain refinement and precipitation hardening of these elements in the form of carbides, nitrides or carbonitrides [11-13].

1.3 Metallurgy

For best properties it is essential to disperse the nanoparticles homogeneously into the system. Take the production of HSAL steels as the example, the conventional metallurgy used to produce HSLA steels was primarily ingot metallurgy (I/M). I/M mainly involves mixing of the molten metal and the solid reinforcement, solidification and subsequent heat treatment [14]. A schematic description of the setup apparatus of I/M is shown in Figure. 1[15]. With advantages of simple operation and quick production, I/M was widely used as the main processing approach to produce metal alloy. However, this conventional metallurgy approach was proved to have poor or heterogeneous dispersion of the alloyed elements, which further restrains their widespread applications [16, 17].

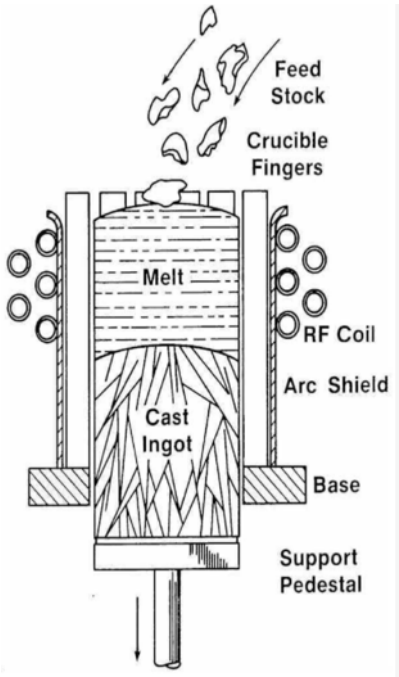

Figure. 1 A simple schematic that shows the apparatus of ingot metallurgy.

Thereafter, powder metallurgy (P/M) was developed to solve this problem and has been more frequently used to produce HSLA steels with improved precipitates distribution and lower cost [18-20]. P/M is a multi-step processing method which first involves atomization, powders mixing, cold processing and degassing followed by vacuum hot processing and hot extrusion, as is shown in Figure. 2[21]. This improved alloying technique, combined with advanced post alloying treatments, led to the development of another major family of steel alloys, called oxide dispersion strengthened (ODS) steels [22]. Their superior mechanical properties and creep resistance at elevated temperature, resulted from the homogeneous distribution of high melting-point metal oxides NPs (Y_2O_3, TiO_2 or Y-O-Ti oxide particles), which make ODS steels the ideal materials for structural application in nuclear fusion reactors [23-25]. Despite the advantages of P/M over I/M, the former alloying technique also showed several limitations, such as potential powder contamination, time-consuming multi-step post-alloying processing and high requirements for the milling conditions and atmosphere purity[23, 26].

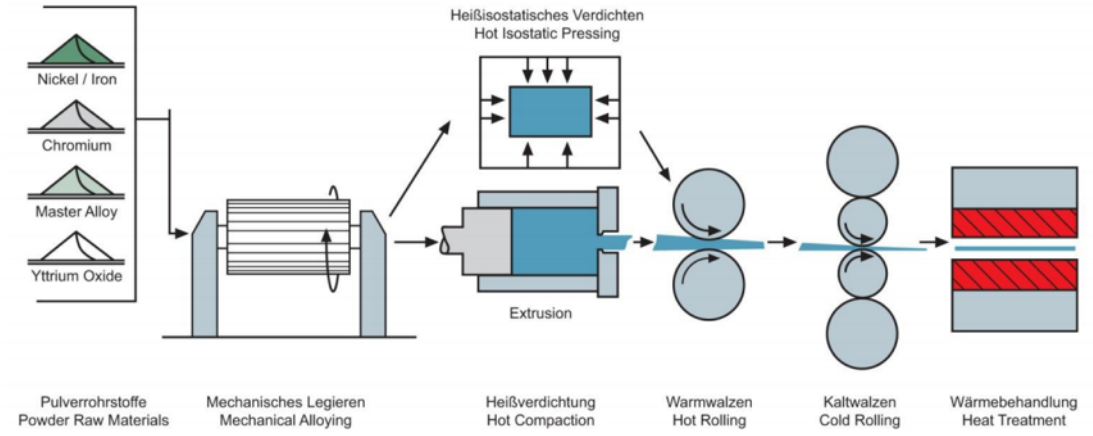

Figure. 2 A schematic of the powder metallurgy (P/M) presented by AR Jones[21].

.

In order to combine the benefits of both metallurgy and avoid their limitations at the same time, we need to prepare alloys through a more simple, efficient and cost-effective method. In this study, we applied nanoparticles aerosol technology during alloying to produce steel alloys with great dispersion of targeted NPs. Briefly, target metal NPs are aerosolized first and carried into the molten steel for alloying, using a lab-scale manufacturing model system designed and installed in our lab, as shown in Figure 3.

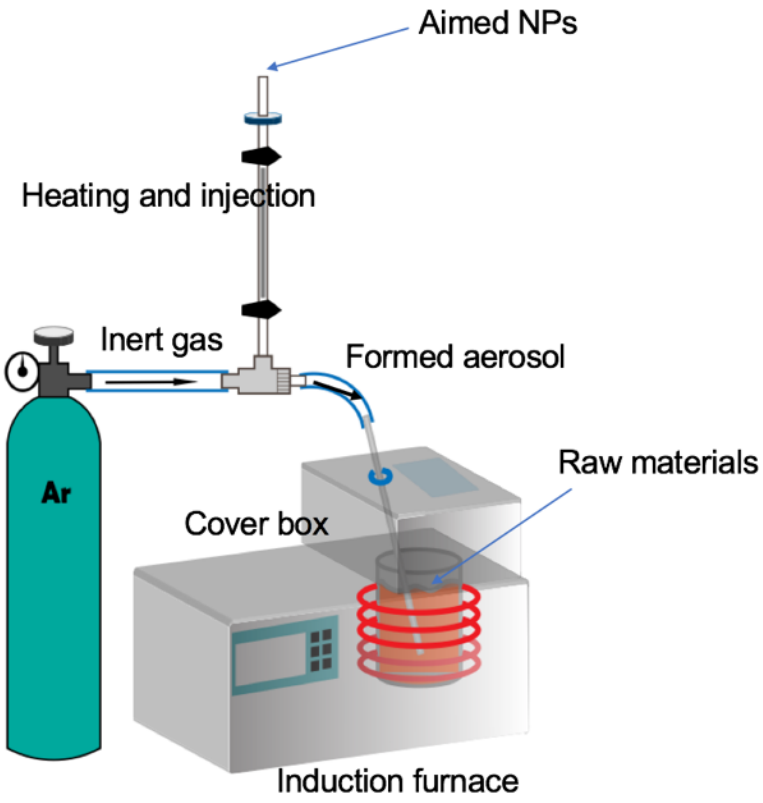

Figure. 3 A schematic of Nanoparticle-Aerosol Technology lab-scale manufacturing system.

REFERENCES

[1] M Kumari, S Gupta, AJ Lakshmi, J Prakash, *Food Chemistry*, **86(2)**: 217-222 (2004).

[2] Kuligowski, J. and Halperin, K. M., *Archives of environmental contamination and toxicology*, **23(2)**:211-215 (1992).

[3] TENG, Huan-bo, Zai-xin FENG and Zhi-min ZHANG, *Light Alloy Fabrication Technology*,**10**: 003 (2006).

[4] Montemarano, T. W., B. P. Sack, and J. P. Gudas, *Journal of Ship Production* **2(3)**: (1986).

[5] R.Z. Valiev M. Yu. Murashkin and I. Sabirov, *Scripta Materialia* , **76**:13–16 (2014).

[6] S. Ukai, M, Harada, H. Okada, M. Inoue, S. Nomura, S. Shikakura, K. Asabe, T. Nishida and M. Fujiwara, *Journal of Nuclear Materials*, **204**:65-73 (1993).

[7] Mann, Surinder. "Nanotechnology and construction." *Nanoforum Report,* 55 (2006).

[8] Raabe D, Ponge D, Dmitrieva O, Sander B, *Scripta Materiali,* **60**:1141-4 (2009).

[9] J. Fernández, S. Illescas, J.M. Guilemany, *Materials Letters*, **61**:2389-2992 (2007).

[10] P.C.M. Rodrigues, E.V. Pereloma, D.B. Santos, *Mater. Sci. Eng. A*, **283**:136–143 (2000).

[11] J.G. SPEER, J.R. MICHAEL and S.S. HANSEN, *METALLURGICAL*

TRANSACTIONS A, **18A**: 211-222 (1987).

[12] Wenhao Zhou, Hui Guo, Zhenjia Xie, Xuemin Wang, Chengjia Shang, *Pure Appl.Chem*, **587**:365-371 (2013).

[13] S.S. HANSEN, J.B VANDER SANDE and MORRIS COHEN, *METALLURGICAL TRANSACTIONS A*, **11A**: 387-402 (1980).

[14] Yong Li, Terence G. Langdon, *Mater. Sci. Eng. A*, **245**:1-9 (1998).

[15] Theodore F. Ciszek, U.S. Patent, 4,572,812, 1986.

[16] Show B, Veerababu R, Balamuralikrishnan R, Malakondaiah G, *Materials Science and Engineering: A*, **527**:1595-604 (2010).

[17] Li Y, Wilson J, Craven A, Mitchell P, Crowther D, Baker T, *Materials science and technology*, **23**:509-18 (2007).

[18] Mora E, Garcés G, Onorbe E, Pérez P, Adeva P, *Scripta Materiali,*. **60**:776-9 (2009).

[19] Xie Z, Liu R, Fang Q, Zhou Y, Wang X, Liu C, *Journal of Nuclear Materials*, **444**:175-80 (2014).

[20] Albiter A, Bedolla E, Perez R, *Materials Science and Engineering: A*, 328:80-6 (2002).

[21] M.K. Miller, K.F. Russell, D.T. Hoelzer, *Journal of Nuclear Materials*, **351**:261–268 (2006).

[22] R.L. Klueh, J.P. Shingledecker, R.W. Swindeman, D.T. Hoelzer, *Journal of Nuclear Materials*, **341**:103-114 (2005).

[23] Suryanarayana C, Ivanov E, Boldyrev V, *Materials Science and Engineering: A*, **304**:151-8 (2001).

[24] Hoelzer DT, Bentley J, Sokolov MA, Miller MK, Odette GR, Alinger M, *Journal of Nuclear Materials,* **367**:166-72 (2007).

[25] El-Genk MS, Tournier J-M, *Journal of Nuclear materials*, **340**:93-112 (2005).

[26] Suryanarayana C, *Progress in materials science*. **46**:1-184 (2001).

CHAPTER 2

2. FEASIBILITY OF NANOPARTICLE-AEROSOL TECHNOLOGY USING CAST IRON

2.1 Introduction

In this chapter, we first present the buildout of the lab-scale alloy manufacturing system, and then present preliminary experiments for the preparation of alloys using selected nanoparticles (W and Ti) and raw material (grey cast iron), followed by the attempt to establish corresponding processing and characterization methods. The purpose of this work was to verify the practicability of the Nanoparticle-Aerosol Technology and identify suitable ways to characterize the products. This lab-scale manufacturing system consists of three parts, a lab-scale, bench top induction furnace with a circular water cooling system to heat the raw materials and which can also help the mixing of injected nanoparticles in the molten metal fluid through the electromagnetic stirring caused by the magnetic field [1]. Secondly, a customized furnace cover with an observation window and an injection port to prevent the oxidation. The key part of this system is the aerosolizer which mixes the nanoparticles and inert gas (Argon) to form the aerosol and transport it to the metal fluid to finish the injection. The design of our aerosolizer

followed the one that was previously described by Tiwari et al [2]. For the very first phase, cast iron was chosen as the raw materials in that this Fe-C-Si alloy offers the unique combination of low cost and engineering versatility. With the special composition (2-4% C and 1-3% Si content), cast iron is around the eutectic point and thus has lower melting temperature ranging from 1150 to 1200 °C, compared to about 1500 °C for low carbon steel and pure iron [3]. The cast iron has good thermal conductivity, low modulus of elasticity, castability and machinability which make it the ideal material for the preliminary tests. As to the nanoparticles, tungsten and titanium, were chosen since their addition results in high performance alloys [4-6]. Moreover, it has been reported that tungsten carbide exhibited great solubility in iron [7] which might help to induce improvements in morphology, grain structure, elemental distribution and mechanical properties all of which will make it easier to validate the usefulness of the Nanoparticle-Aerosol Technology.

2.2 Experimental Section

2.2.1 Materials

For ease of processing, gray cast iron rods, which were purchased from McMaster-Carr Supply Company (US), were used as the raw materials for preparing alloys. Several nanoparticles (NPs) have been tested including tungsten NPs (40-60 nm) and titanium NPs (70 nm), purchased from US Research Nanomaterials, Inc.

2.2.2 Apparatus

To carry out the experiments a bench top processing apparatus was especially designed and built for the project *(Figure. 4)*.

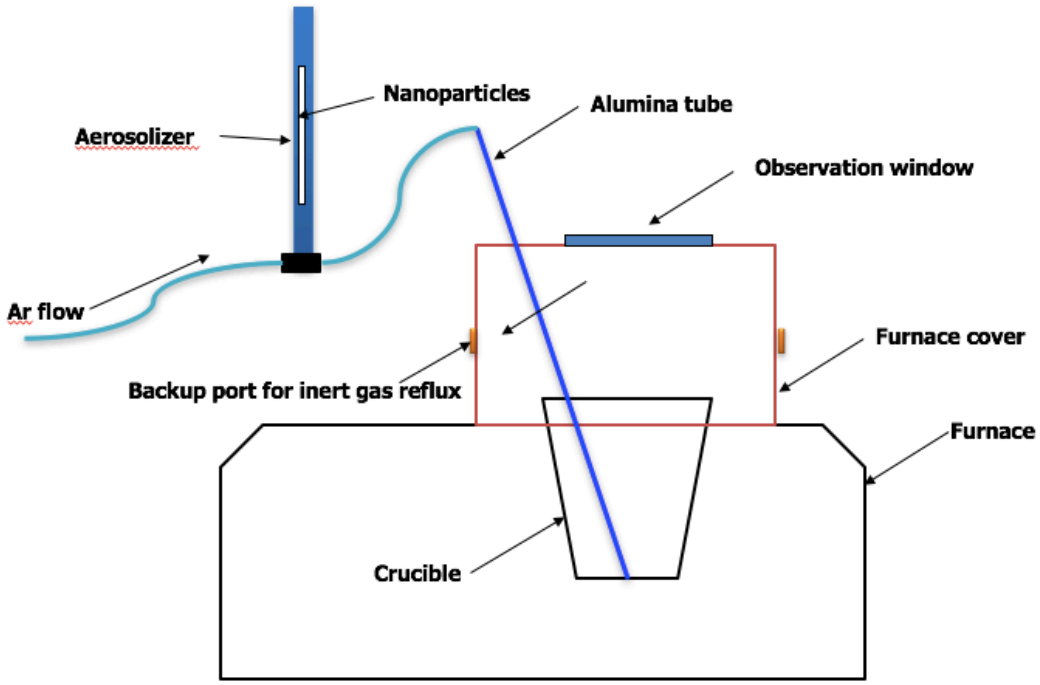

Figure. 4 Schematic of lab-scale furnace and aerosolizer processing system. The apparatus includes containment for minimizing oxidation during processing.

The lab-scale, bench top induction furnace with a circular water cooling system has been purchased from RDO Induction Inc. (Figure. 5, 6). Accessories like ceramic tubes, and ceramic crucibles, graphene mold were procured as well.

Figure. 5 Image showing the induction furnace and the cooling system.

Moreover, a furnace cover with an observation window and an injection port was customized and installed to prevent the molten steel and NPs from oxidation. (Figure. 6(a)).

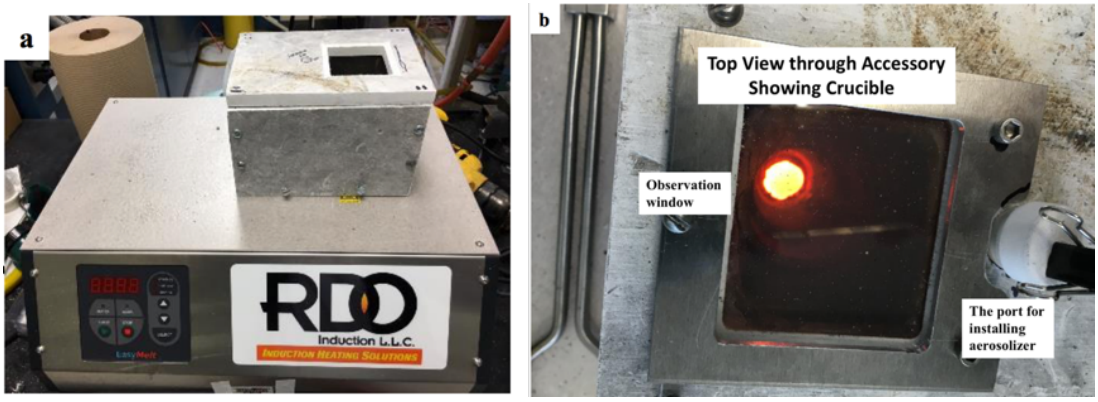

Figure. 6 (a) Induction furnace with the cover box. (b) Image showing top view of the cover box.

The design of our aerosolizer followed that previously described by Tiwari et al.[18] (Figure. 7(a)). This aerosolization system holds the NPs between two valves and the argon helps carry the NPs released by opening the lower valve (Figure. 7(b)). The NPs aerosol is injected into the molten metal fluid in the crucible from the top using alumina tubes.

a

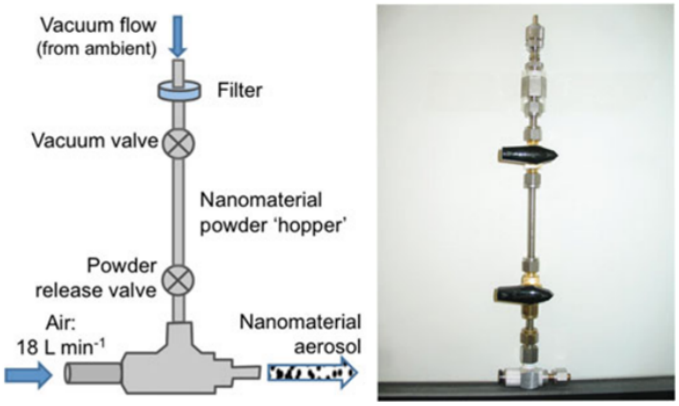

b

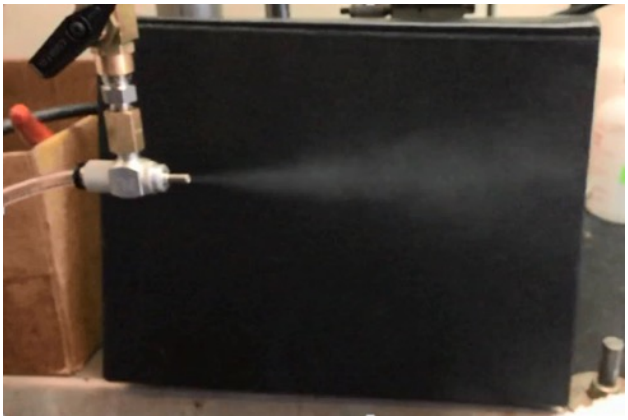

Figure. 7 Schematic (a) and actual aerosolizer (b) built for the lab-scale manufacturing system.

2.2.3 Processing

All raw materials were cut to smaller chips before alloying. Specifically, 50-80 grams of cast iron was weighed and then placed in the ceramic crucible, followed by flushing by argon for at least 5 min before the injection to minimize oxidation. Certain amount of

NPs were weighed and carefully packed into the aerosolizer. For melting the raw material, power output was maintained at 65% for cast iron until all chips were completely molten. Then the aerosolizer was turned on for the injection while the power output is turned down by 10% during the injection, which lasts for around 5 to 10 minutes while the aerosolizer was being shaken to prevent clogging of the NPs. After the injection, the molten steel was poured into graphite molds and placed back in the crucible for a brief heat treatment for 30 min using 20% of the furnace power. After the heat treatment, the alloys were cooled down to room temperature before any other processing. Pristine samples were also processed similarly but in the absence of nanoparticles for comparative purposes (control samples). Alloy samples were processed to 25x5x3 mm rectangular shaped specimens and coarsely polished at the machine shop. Further fine polishing of samples was performed using silica carbide sheets from 180 to 800 grit polishing paper and finished with a final polishing using 1 μm alumina. All polished samples were then washed by water and methanol using a sonicator and dried. The final metallographic specimens were prepared by etching the polished cast iron alloys for 15-20s using 5% Nital solution (mixture of nitric acid and ethanol) . Figure. 8 shows the samples before and after etching.

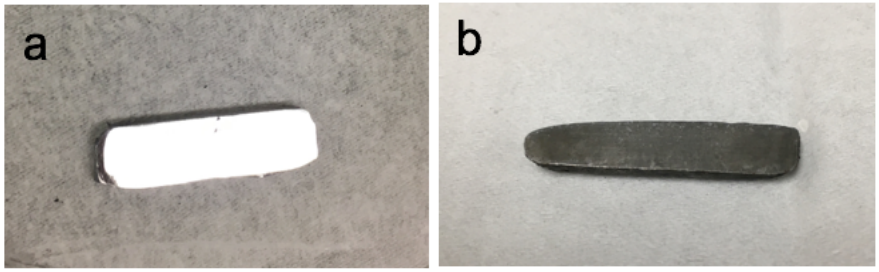

Figure 8. Sample a) before etching and b) after etching.

2.2.4 Characterization

In order to evaluate the dispersion of the metal NPs in the new alloys, a LEO 1550 Field Emission Scanning Electron Microscope (FESEM), coupled with an Oxford X-Max SDD Energy-dispersive X-ray spectroscopy (EDS), was employed. Cross-sections of the alloys were scanned for elementary analyses and high resolution chemical mapping. For metallography studies, fine-polished cast iron alloys were subjected to etching by Nital etchant for 30 seconds. The etched surface was then washed and observed using an Olympus optical microscope. Hardness of different samples was measured using a Rockwell hardness tester based on Rockwell C standard. A thin slice was cut from each alloy sample and multiple sampling points were measured based on the design shown in Figure. 9. After the measurements, a 3D surface map of hardness is drawn to estimate the effect of dispersion of NPs on hardness.

Figure 9. Design of the multi-point sampling for hardness test.

2.3 Results and Discussion

2.3.1 Production of Cast Iron Alloys

Using cast iron as the parent material, several alloys have been prepared by injecting different amounts of tungsten (W) and titanium (Ti) NPs. In order to magnify the produced changes, we started first with the introduction of higher amounts of nanoparticles. Tungsten NPs (40-60 nm), which have much higher density (19.3 g/cm^3) than titanium (4.506 g/cm^3) and better solubility in iron were used first. Initially, the concentrations of W NPs ranged from 10 to as high as 15 wt%. We note that these are *nominal concentrations*, since some loss of NPs might happen during the injection. Based on the encouraging results from 10-15 wt% W-cast iron alloy products, the concentration of W NPs was lowered to more usual levels so as to approach the industrial standard for preparation of W-contained alloy. Moreover, because the super high density of W NPs and the inevitable loss during injection, 2.5 and 5 wt% were finally selected as the concentrations for injected W NPs. For Ti NPs, for the same considerations and because of its relatively low density, samples containing 0.5 to 2.5 wt% of initial nominal concentration were prepared. Pristine sample, the pure iron control was also prepared under the same processing condition for comparison.

2.3.2 Optical Metallography

The metallography and surface morphology of pure iron control, 10 wt% and 15 wt% W-based iron alloys are shown in Figure 10. After melting in the furnace and recasting into

the mold, followed by quick water cooling, the cast iron control sample shows a typical lath martensite microstructure. Austenite was not that distinguishable due to the relatively low content and fine size. In contrast, Figure. 10(b), 10(c) showed that the 10 wt%, 15 wt% W-based iron alloy consisted of predominantly pearlite and network-like cementite in small amount. The tungsten-iron alloys exhibited a significant modified microstructure compared to the control. With the addition of W NPs, the alloy microstructure shows significant refinement and homogeneous distribution. Moreover, with increasing amount of injected W NPs (10% to 15%), the grain size was further refined while the distribution of the microstructure appeared more regular and even.

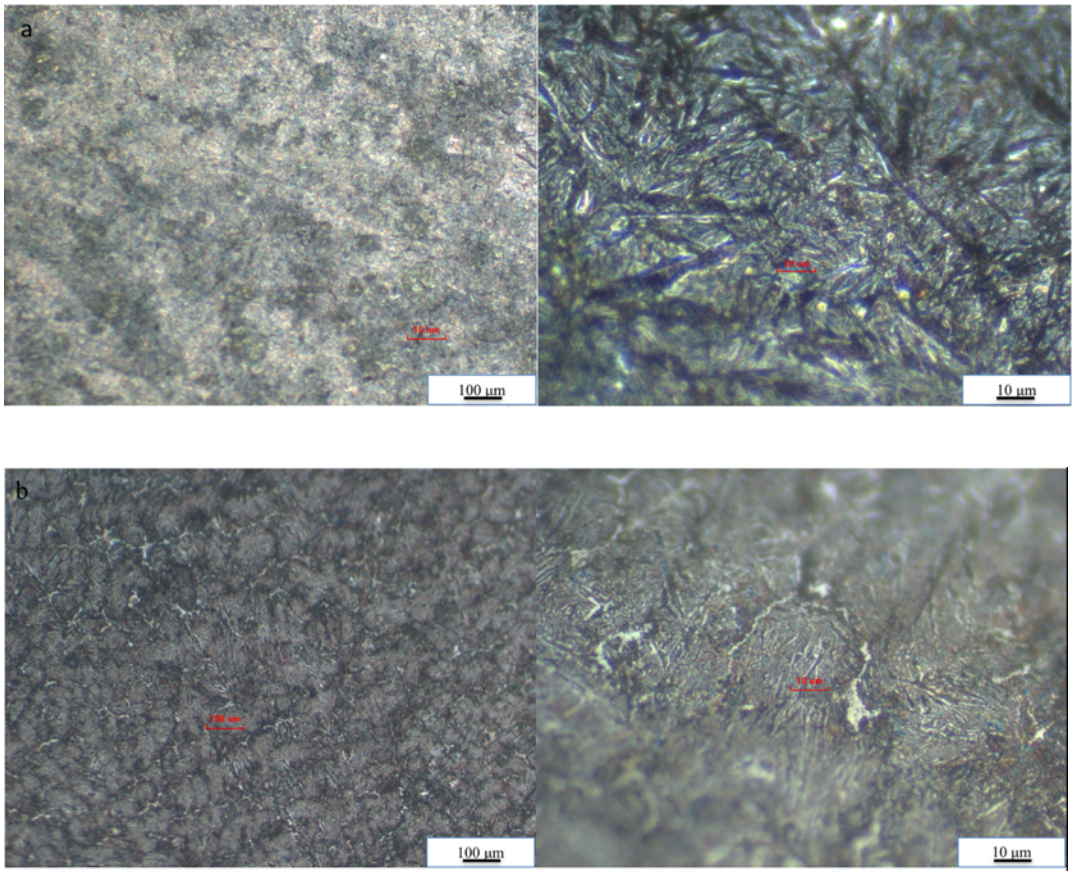

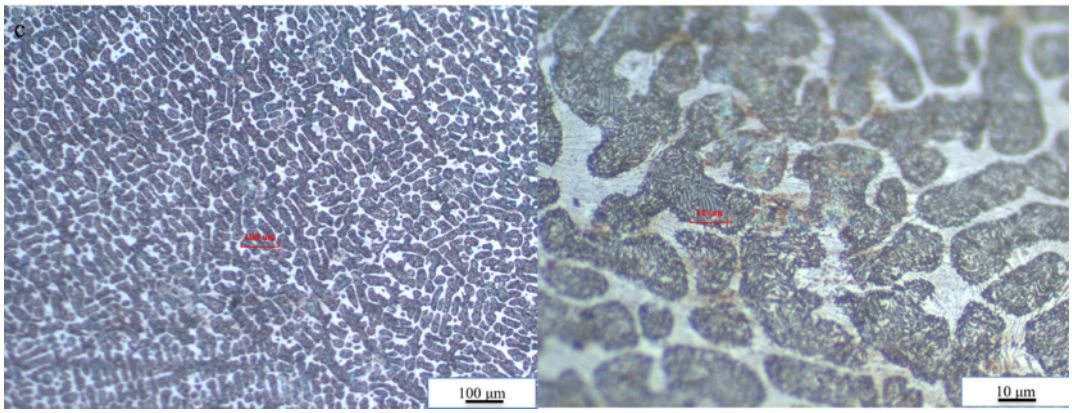

Figure 10. Optical micrograph of the as-cast samples with different W content: a) 0 wt% b) 10 wt% and c)15 wt%.

Based on the above results from high concentration samples, lower concentration alloys based on W and Ti were prepared. For W based iron alloy, 2.5 and 5 wt% were selected as the concentrations. As to Ti NPs, which has relatively low density, samples containing 0.5, 1 and 2.5 wt% particles were prepared. Significant change in microstructure with a trend to be more homogeneous were observed as well as shown in Figures 11 and 12.

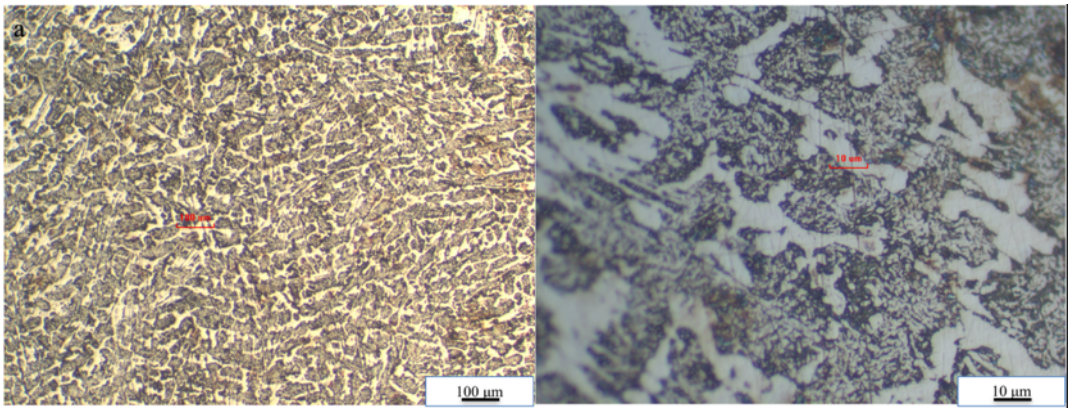

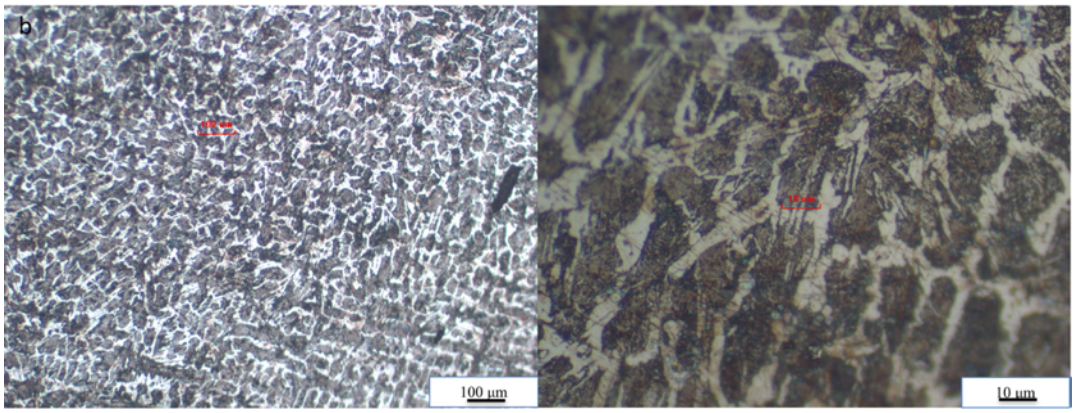

Figure 11. Optical micrographs of the as-cast samples with different W content: a) 2.5 wt% and b) 5 wt%.

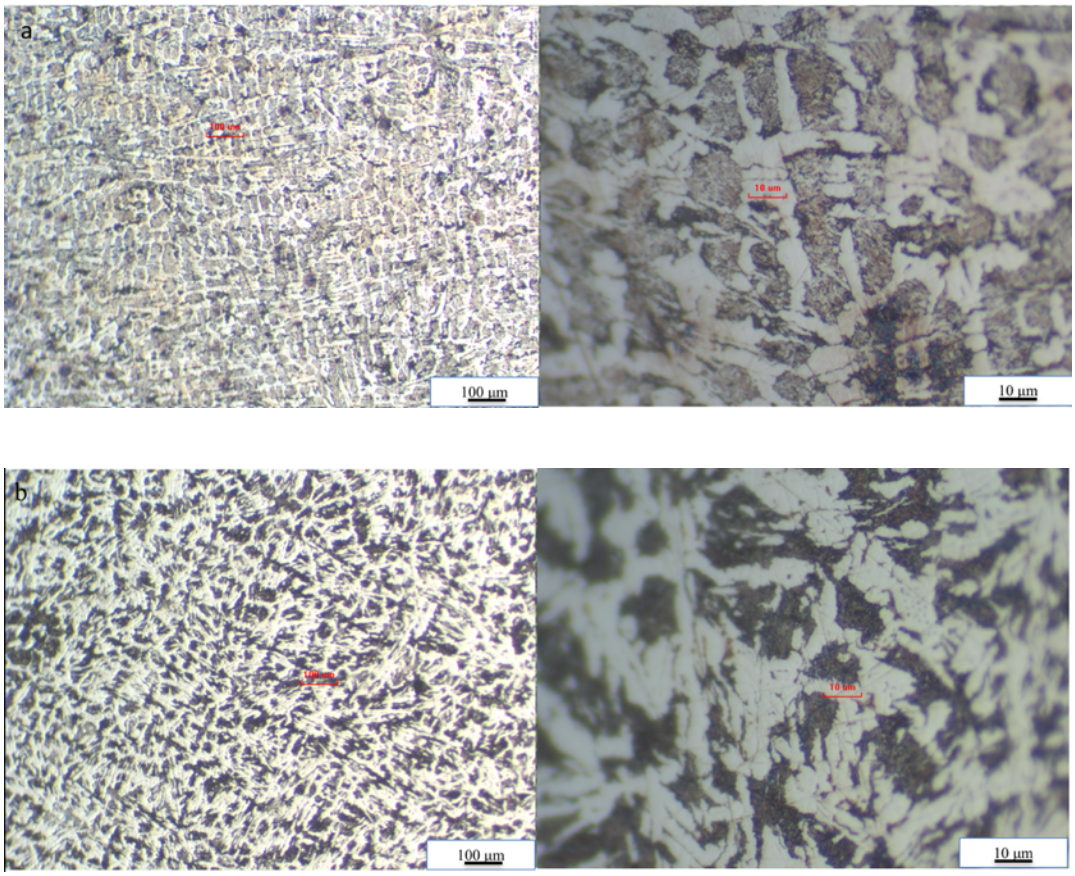

Figure 12. Optical micrograph of the as-cast samples with different Ti content: a) 0.5 wt%, b) 1 wt% and c)2.5 wt%.

2.3.3 Dispersion of Injected Nanoparticles

The promise of nanotechnology is that it can develop novel materials with revolutionary physical, chemical, mechanical or optical properties by controlling or modifying materials at the molecular or nanometer scale. However, the nanoparticle dispersion into the matrix is the essential factor which needs to be taken into account. Conventional production method, ingot metallurgy (I/M) offers low cost and ease of operation, but it always results in poor or heterogeneous dispersion of the alloyed elements, which limits more applications. In order to evaluate the dispersion of the metal NPs in new alloys, a LEO 1550 Field Emission Scanning Electron Microscope (FESEM), coupled with an Oxford X-Max SDD Energy-dispersive X-ray spectroscopy (EDS), was employed to scan the cross-sections of the alloys for elementary analyses and high resolution chemical mapping.

Figure 13 shows the SEM and EDS images of the W-based iron alloy samples. Combined with the optical metallography from Figure 10,11 and the surface morphology from SEM, it is clear that with increasing amounts of injected W NPs, the grain structure became more regular and homogeneous while the grain size decreased. The injected W NPs appear to facilitate the formation of different grain structures (compared to the control samples). This phenomenon is clearly observed in alloys with higher W NPs content. In the EDS elemental mapping, shown in Figure 13, the bright red spots represent the real signal of W nanoparticles. The latter is confirmed using the EDS spectra which showed a clear peak for W in Figure 1 while the control sample with no W NPs injected showed no peak for W (Figure 14 (a)). Thus, the EDS results confirm that W NPs were uniformly distributed into the cast iron matrix. It is worth mentioning that, with increasing amount

of W NPs, the corresponding number of bright red spots on elemental mapping increases. Moreover, W NPs preferred precipitating around the grain boundary. As shown in Figure 14, the EDS spectra not only confirm the presence of W but also carbon, which suggests the presence of tungsten carbide. This can be further supported by the results of optical metallography. For the cast iron with high content of carbon, after being processed at rapid cooling rate, the formation of graphite will not occur, instead, austenite dendrites start to form. During the solidification, the interdendritic area remains carbon-rich and finally solidified in the form of iron carbide, which was named cementite [8]. Therefore, with the W NPs mainly precipitated in the cementite area which is also carbon-rich area, it is reasonable to suggest that the W precipitates in the form of tungsten carbide. Moreover, the existence of WC around the grain boundary can further account for the refinement of the grain size with increasing amount of injected W NPs.

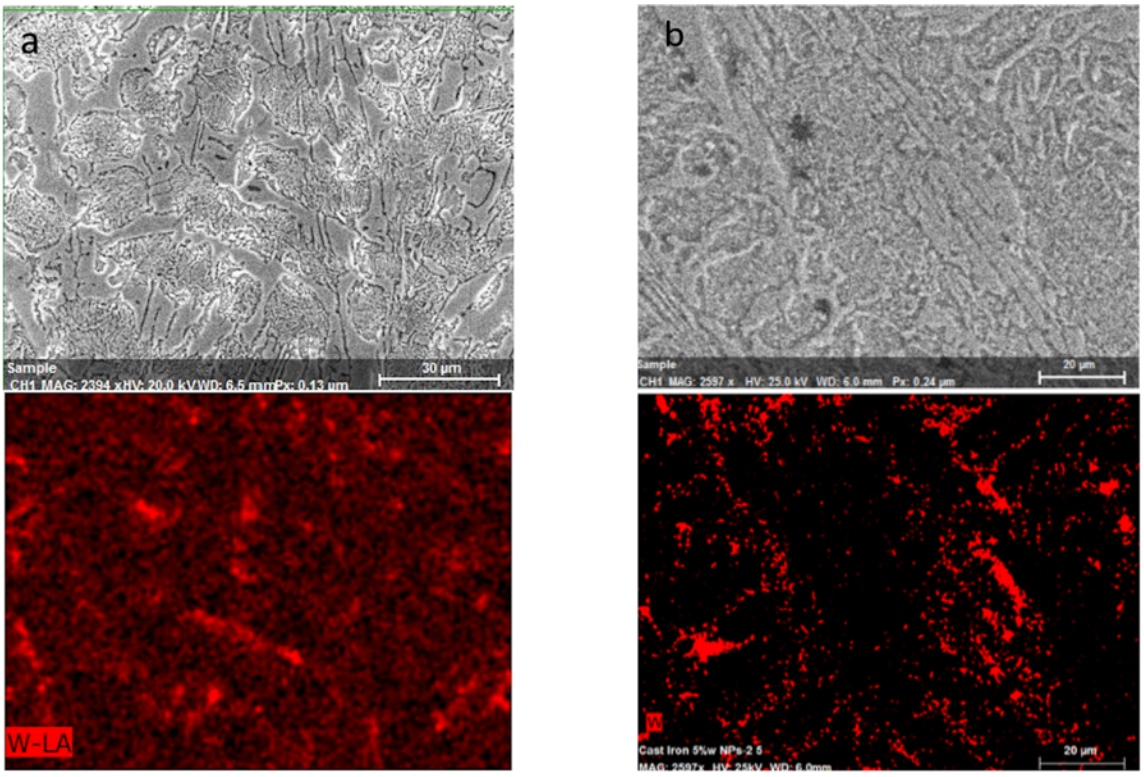

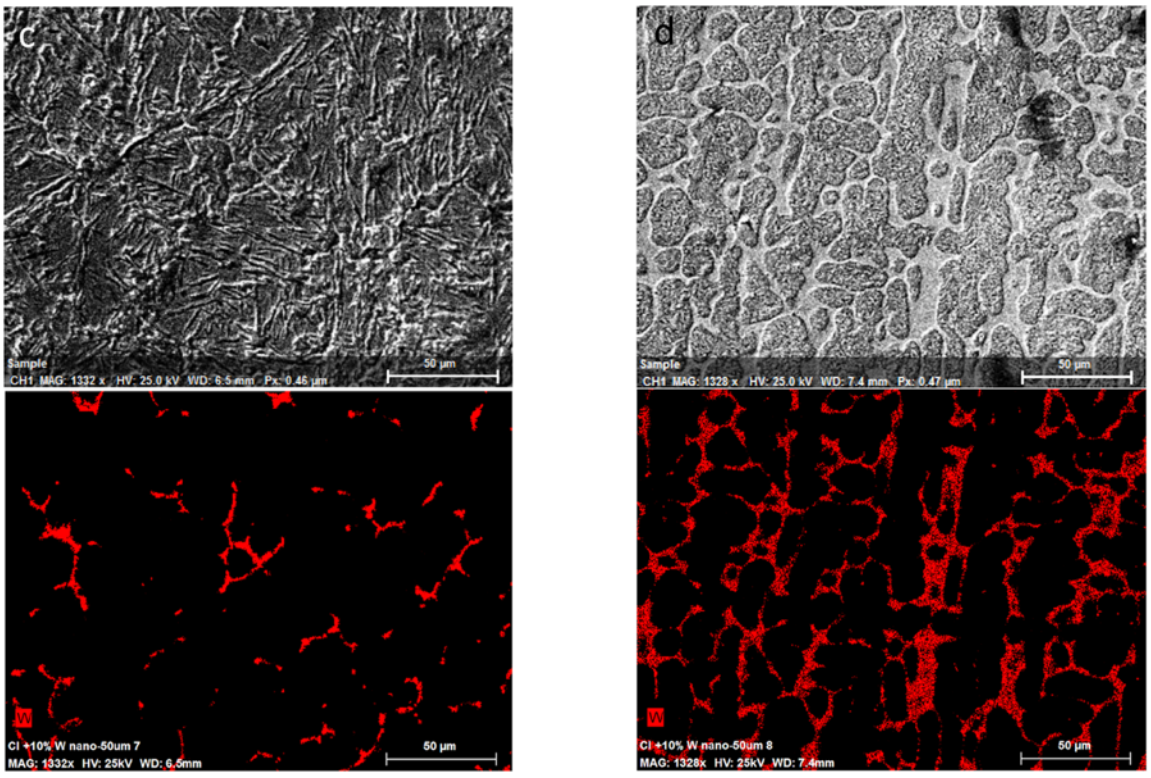

Figure 13. Distribution/morphology of W NPs for cast iron samples injected with a)2.5 wt%, b)5 wt%, c)10 wt% and d)15 wt% W NPs.

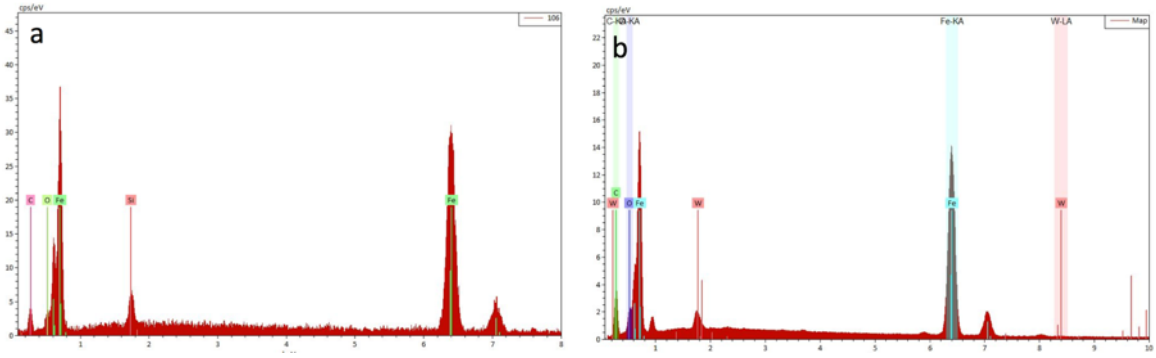

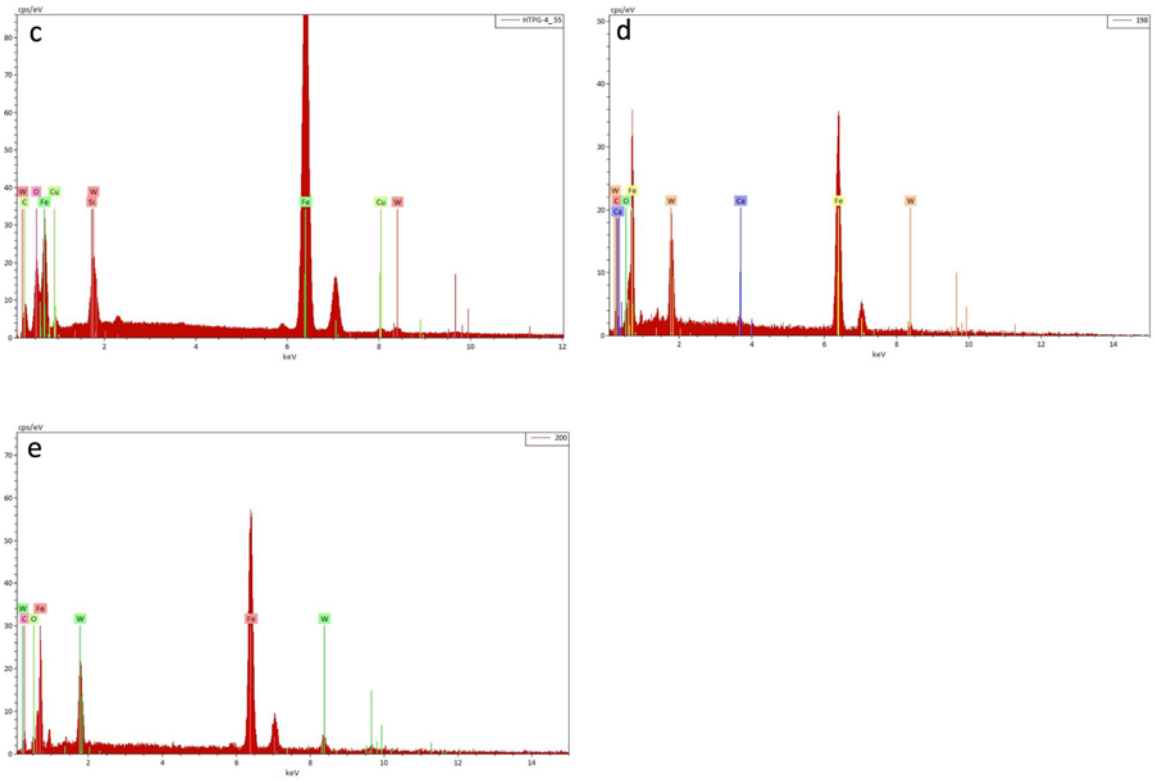

Figure 14. EDS spectra for cast iron alloy samples injected with a) 0 wt%, b)2.5 wt%, c)5 wt%, d)10 wt% and e)15 wt% W NPs.

For the Ti-based iron alloy, though the clear distribution around the grain boundary was not observed, the bright red spots on the elemental mapping (Figure 12) and the peak of Ti in EDS (Figure. 13) also confirmed the successful injection of Ti NPs.

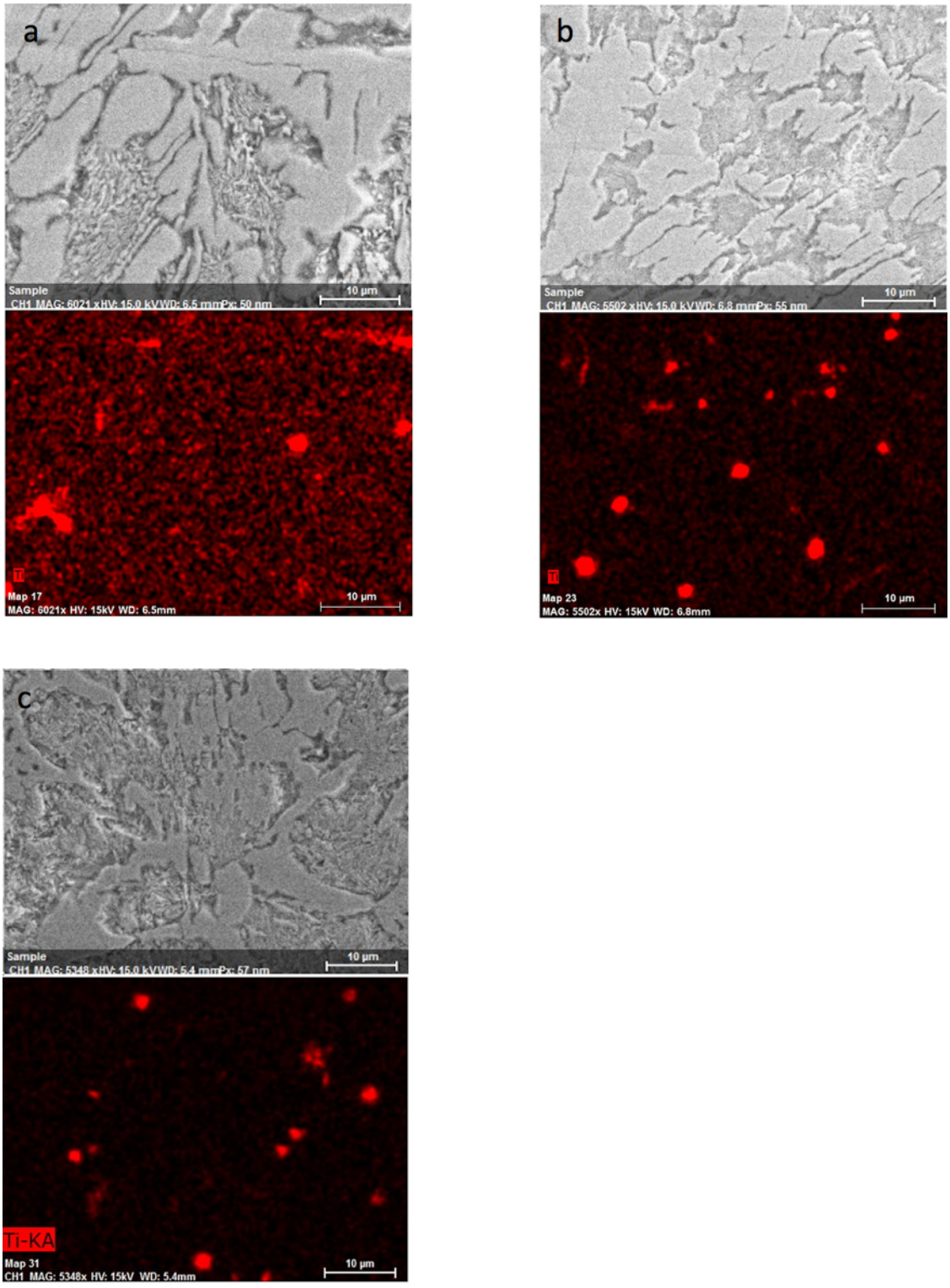

Figure 15. Distribution/morphology of Ti NPs for cast iron samples injected with a)0.5 wt%, b)1 wt% and c)2.5 wt% Ti NPs.

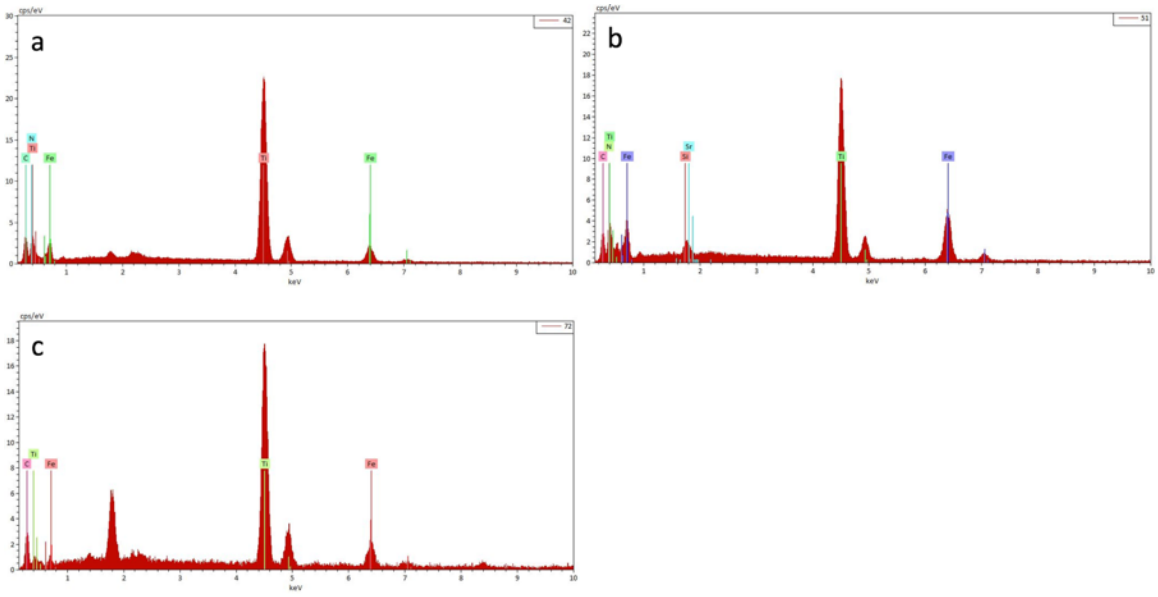

Figure 16. EDS spectra for cast iron samples injected with a) 0.5 wt%, b) 1 wt% and c) 2.5 wt% Ti NPs.

2.3.4 Hardness Test

The hardness measurements of pristine cast iron steel control and other samples with different nanoparticles and different injection contents were performed using a hardness tester, in accordance with Rockwell C standard and micron-indentation. The results were listed in Table 1. At least five measurements were taken for each sample to improve statistics.

Table 1. Hardness (both Rockwell C and micro-indentation measurements) of alloys with W and Ti NPs.

	Hardness (Rockwell C)	Hardness (micro-indentation)
Cast iron (control)	56.5 ± 0.6	523.3 ± 15.1

Cast iron-2.5% W	51.7 ± 0.4	525.9 ± 12.1
Cast iron-5% W	41.5 ± 1.0	486.2 ± 17.4
Cast iron-10% W	42.7 ± 1.0	416.0 ± 9.4
Cast iron-15% W	48.6 ± 0.1	511.9 ± 2.2
Cast iron-0.5% Ti	50.4 ± 0.4	527.7 ± 15.0
Cast iron-1.5% Ti	52.5 ± 0.3	623.7 ± 22.5
Cast iron-2.5% Ti	49.3 ± 0.7	563.3 ± 14.7

In general, iron alloys with addition of W and Ti resulted in small loss of hardness. The very high content of silicon in cast iron makes it very hard and a possible explanation for the loss of hardness might be defects or cracks due to the excess injection of particles. However, it was recognized that for the W-based samples, with increasing amount of injection, the hardness would increase accordingly which was consistent with the grain refinement from optical metallography.

Another 8 sets of hardness measurements based on Rockwell C were taken from the test set shown in Figure 9. With the measurements, a 3D surface map of hardness is drawn for estimating the dispersion of NPs in the matrix. As shown in Figure 17, the 3D plots appear relatively smooth, which indicated the even distribution of hardness on the alloys and thus effectively further confirmed the homogeneous distribution of alloyed NPs.

A

Control-water cooled

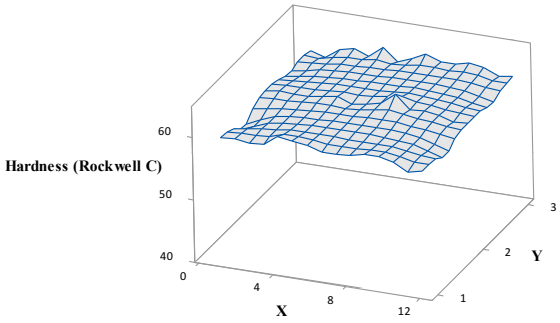

B

Cast iron control-air cooled

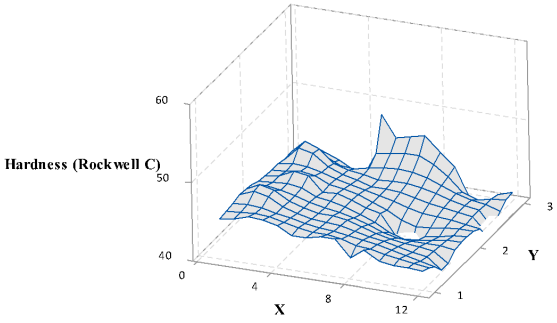

C

Hardness of CI with 1% Ti

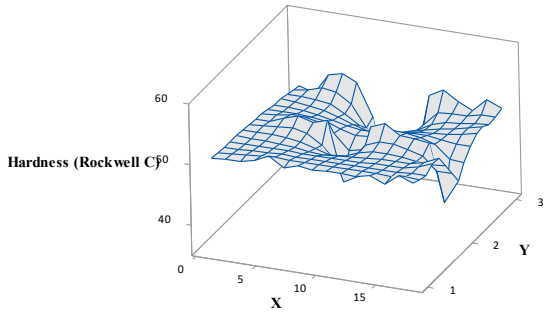

D

Hardness of CI with 2.5% Ti

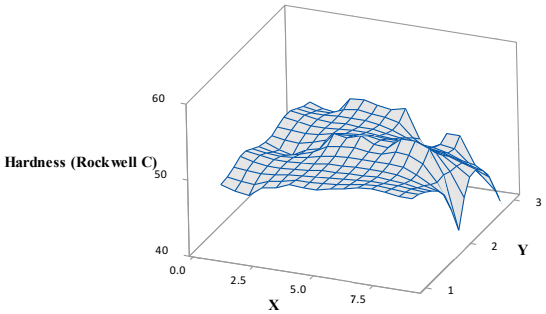

E

Hardness of CI with 2.5% W NPs-water cooled

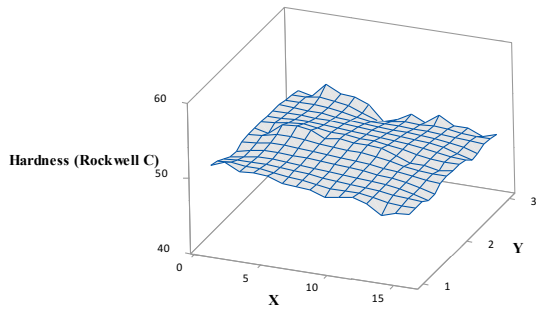

F

CI with 2.5% W-air cooled

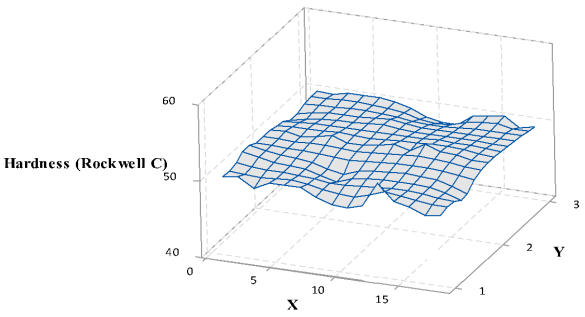

G

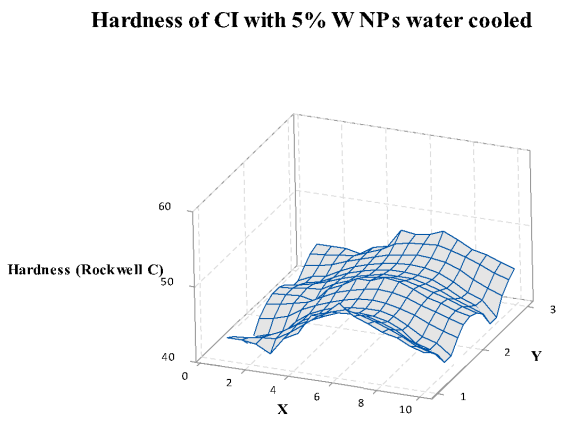

H

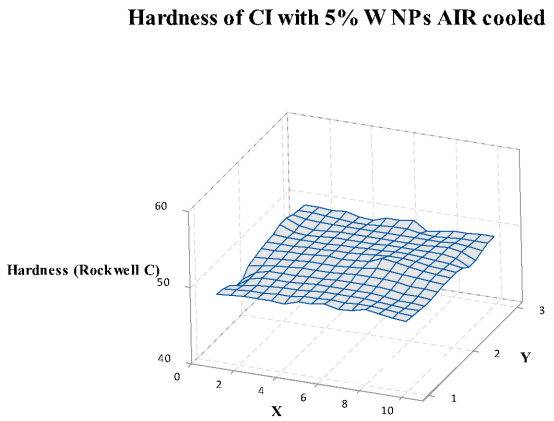

Figure 17. Hardness measurements of pristine cast iron (control) and alloys containing Ti or W NPs.

2.4 Conclusions

A lab-scale alloy manufacturing system, which consists of three parts a bench top induction furnace with a circular water cooling system, customized furnace cover box, and an aerosolizer is demonstrated. Experiments were conducted using cast iron as the raw material while the W and Ti NPs were chosen as the alloying elements. In addition to the preparation post-processing (grinding and etching approach) and characterization methods (optical metallography, SEM and EDS) were also established. The new alloy samples exhibited significantly altered microstructures (grain size and morphology) compared to the controls. Especially for those W-based iron alloys, which have relatively high volume injection, the grain size of alloy shows significant refinement and homogeneous distribution. Moreover, with increasing amount of injected W NPs (2.5% to 15%), the grain size was further refined while the distribution of the microstructure appeared more regular and even. Results from elemental mapping and EDS spectra

further confirmed the presence of injected W NPs and the form (tungsten carbide) it existed in the allo, which accounts for the refinement of grain structure. Similar changes were observed when Ti NPs were used. The hardness results also indicate good homogeneity and improvement of mechanical properties obtained using this novel approach.

REFERENCES

[1] Bowen Xiong, Changchun Cai, Hong Wan, Baiping Lu, *Materials and Design*, **32**:2978–2982 (2011).

[2] Tiwari, Andrea J., Caleb G. Fields, and Linsey C. Marr, *Aerosol Science and Technology*, **47(11)**: 1267-1275 (2013).

[3] Elliott, Roy. *Cast iron technology*. Butterworth-Heinemann, 1988.

[4] Yezhe Lv, Yufu Sun, Jingyu Zhao, Guangwen Yu, Jingjie Shen and Sumeng Hu, *Materials and Design*, **39**:303-308 (2012).

[5] Rong Zhou, Yehua Jiang and Dehong Lu, *Wear*, **255**:134–138 (2003).

[6] Seo, M., Hultquist, G., Leygraf, C. and Sato, N., *Corrosion Science*, ***26*(11)**: 949-960 (1986).

[7] Erik J. Pavlina, John G. Speer and Chester J. Van Tyne, *Scripta Materialia*, **66**:243–246 (2012).

[8] Angus, Harold T., *Cast iron: physical and engineering properties*. Elsevier, 2013.

CHAPTER 3

3.INVESTIGATION ON THE POTENTIAL OF NANOPARTICLE-AEROSOL TECHNOLOGY

3.1 Introduction

The next step involved evaluating the technique with samples based on more complex compositions. The success in applying this method to both W and Ti NPs have suggested the versatility of the approach since these two materials are very different from each other (high density W NPs vs. low density Ti NPs). Accordingly, instead of using cast iron which has low modulus of elasticity, low carbon 1018 steel was chosen as the raw material. 1018 steel is simply iron with 0.18% carbon content. As the most commonly available with cold-rolled steels, it has a good combination of toughness, strength, ductility and comparative ease of machining which makes it a widely used commercial material in daily life and for industrial applications [1, 2]. With respect to additives, Niobium (Nb) was chosen as one of the aimed particles. This choice was made because niobium is the most commonly used alloying element for production of microalloyed steel, a mature commercialized steel [3]. Nb precipitates as carbonitride and induces grain refinement which largely improves the mechanical properties of alloyed steel [4,5]. Secondly, the potential to realize the good dispersion of alloyed agents even when the addition amount is as low as the industrial standard (in most cases, less than 1 wt%) was investigated. Finally, we compare this novel approach and conventional metallurgy. With all the other conditions fixed, Nb alloyed samples were prepared by different alloying methods (regular alloying and aerosolizing) using particles with different sizes (micron and nano scale). Therefore, four different samples were prepared as shown in Table 2.

However, comparisons will mainly focus on the results from samples produced by conventional metallurgy (A) and Nanoparticle-Aerosol Technology (B).

Table 2. Type of nanoparticles and processing for preparing 1018 steel alloys.

Sample	Aimed particles	Alloying method
A	Nb powders (< 45 μm)	Regular alloying
B	Nb NPs (50 nm)	Aerosolizing
C	Nb powders (< 45 μm)	Aerosolizing
D	Nb NPs (50 nm)	Regular alloying

3.2 Experimental Section

3.2.1 Materials

1018 general purpose low-carbon steel (cold drawn) was purchased from McMaster-Carr (Elmhurst, IL) as the raw material. Niobium nanoparticles (Nb, 99.9%, 50 nm) were purchased from US Research Nanomaterials, Inc. (Houston, TX). Niobium powders (< 45 μm, 99.8% trace metals basis) were obtained from Sigma-Aldrich (St. Louis, MO).

3.2.2 Processing

Before alloying, 1018 steel rods were cut to smaller chips and stored under inert gas. 50-80 grams of the 1018 steel chips were weighed and put in the ceramic crucible, which was flushed by argon for 5 minutes. Certain amount of the metal NPs was then weighed and carefully packed in the aerosolizer. After the power was turned on and the steel chips

were completely molten (power output 85%), the aerosolizer was turned on for the injection (power output 75%), which lasted for 5-10 minutes until the injection was finished. After the injection, the molten alloy was poured into the graphite mold and subjected to certain heat treatment in the crucible for variable time, followed by an air cooling process. Alloys were then machined to thin rectangular tablets and subjected to coarse polishing, followed by fine polishing using silicon carbide sheets from 180 to 800 grit paper and final polishing with 1 μm alumina. All polished samples were then washed by water and methanol using a sonicator and dried before further characterization. Metallographic specimens were prepared by etching the polished 1018 steel alloys for 20-25s using 5% Nital solution (mixture of nitric acid ethanol) [6].

3.2.4 Characterization

Grain structure was examined and recorded by Olympus general purpose imaging microscope. In order to evaluate the dispersion of the metal NPs in the new alloys, a LEO 1550 Field Emission Scanning Electron Microscope (FESEM) coupled with an Oxford X-Max SDD Energy-dispersive X-ray spectroscopy (EDS) was used. Hardness measurements were performed using a Rockwell hardness tester based on Rockwell B standard. Multiple sampling points were measured on a thin slice of the alloy cross-section.

3.3 Results and Discussion

3.3.1 Production of 1018 Steel Alloys

To investigate the versatility of the new approach, 1018 steel (low carbon content, high melting point and high modulus of elasticity), which is very different from cast iron, was selected as the raw material with Nb as the alloying particles. Samples were prepared as shown in Table 3. Comparisons were made in terms of particle size and alloying method used. The concentration of the Nb was kept at 0.1 and 0.5 wt%. Analysis focused primarily on samples produced by conventional metallurgy (recipe A) and Nanoparticle-Aerosol Technology (recipe B). In fact, because of the high modulus of elasticity (29700ksi, more than twice of that in cast iron), mixing because of the electromagnetic stirring might be less effective.

Table 3. Nb alloys based on 1018 steel using different compositions and processing

Recipe	0.1 wt%	0.5 wt%
Nb powders (< 45 μm) + Regular alloying	A1	A2
Nb NPs (50 nm) + Aerosolizing	B1	B2
Nb powders (< 45 μm) + Aerosolizing	C1	C2
Nb NPs (50 nm) + Regular alloying	D1	D2

3.3.2 Optical Metallography

The micrograph and surface morphology of pure 1018 steel control, 0.1 wt% and 0.5 wt% Nb-based 1018 steel alloys based on regular alloying and our approach are shown in Figures 18 and 19. With the addition of Nb particles, compared to the control, the grain structures vary depending on processing conditions. With regard to the comparison between samples prepared by conventional metallurgy (A1, A2) and Nanoparticle-Aerosol Technology (B1, B2), the grain structure for samples B1and B2 (Figure 19 a, b) appeared much more homogeneous and regular than that in samples A1 and A2 (Figure 18 b, c) which suggests better dispersion of Nb particles. Nevertheless, even though the change in aspects of micrograph was still significant for 1018 steel alloyed with Nb using our novel approach, the difference was not as large as observed in Chapter 2 for the cast iron alloyed with W and Ti. The difference might be due to the large carbon content difference between 1018 steel (0.18%) and cast iron (2-4%). 1018 steel did not have enough carbon to react with the injected Nb nanoparticles which means the amount of carbide or carbonitride[] would be far less than that in cast iron alloys. It is known that carbide or carbonitride play an important role in changing the morphology and refinement of grain size. However, the homogeneous grain structure can still be achieved in low carbon 1018 steel.

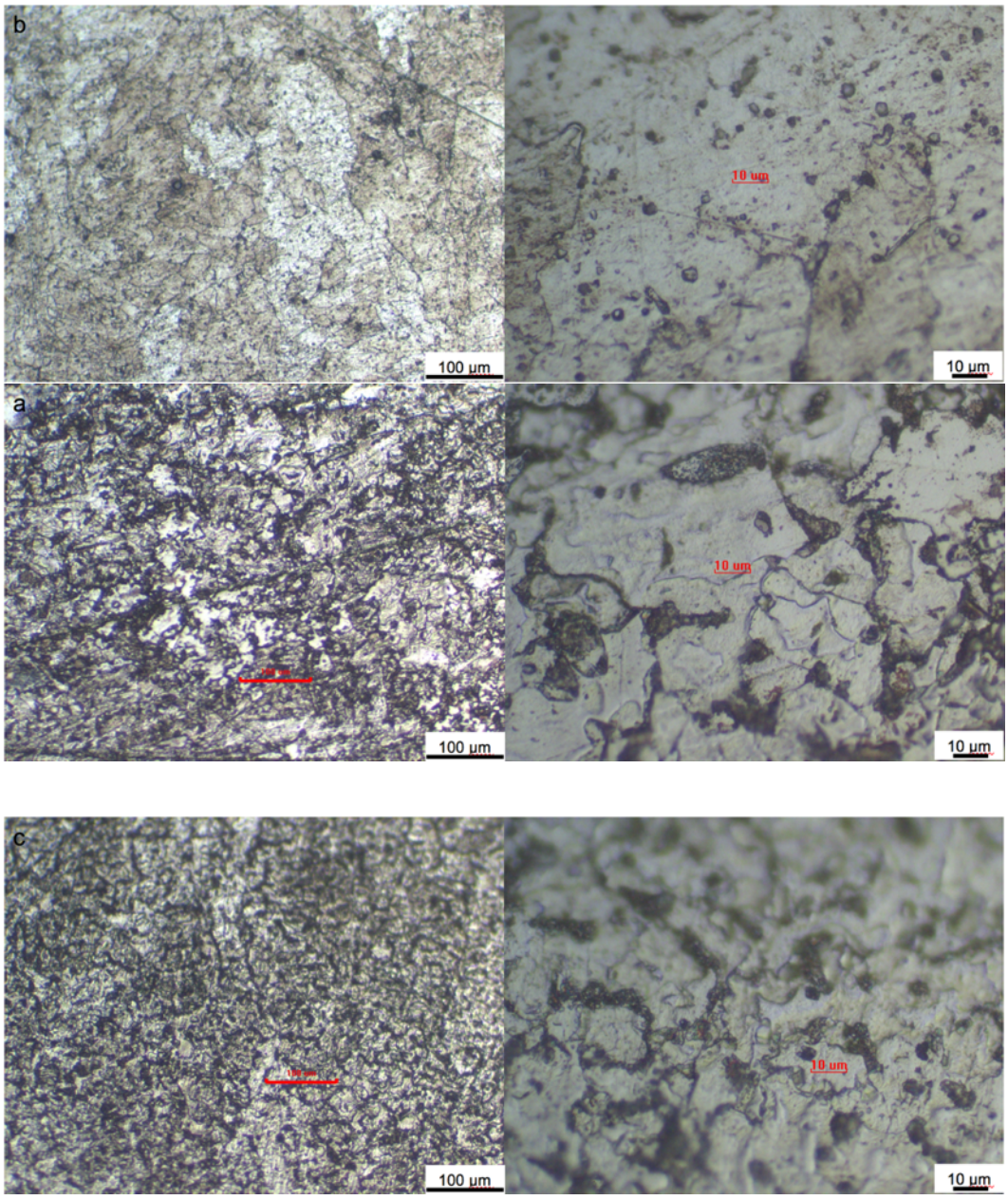

Figure 18. Optical micrograph of a) the plain 1018 steel control and samples produced by conventional metallurgy, A and different Nb content: (b) A1 with 0.1 wt% and (c) A2 with 0.5 wt%.

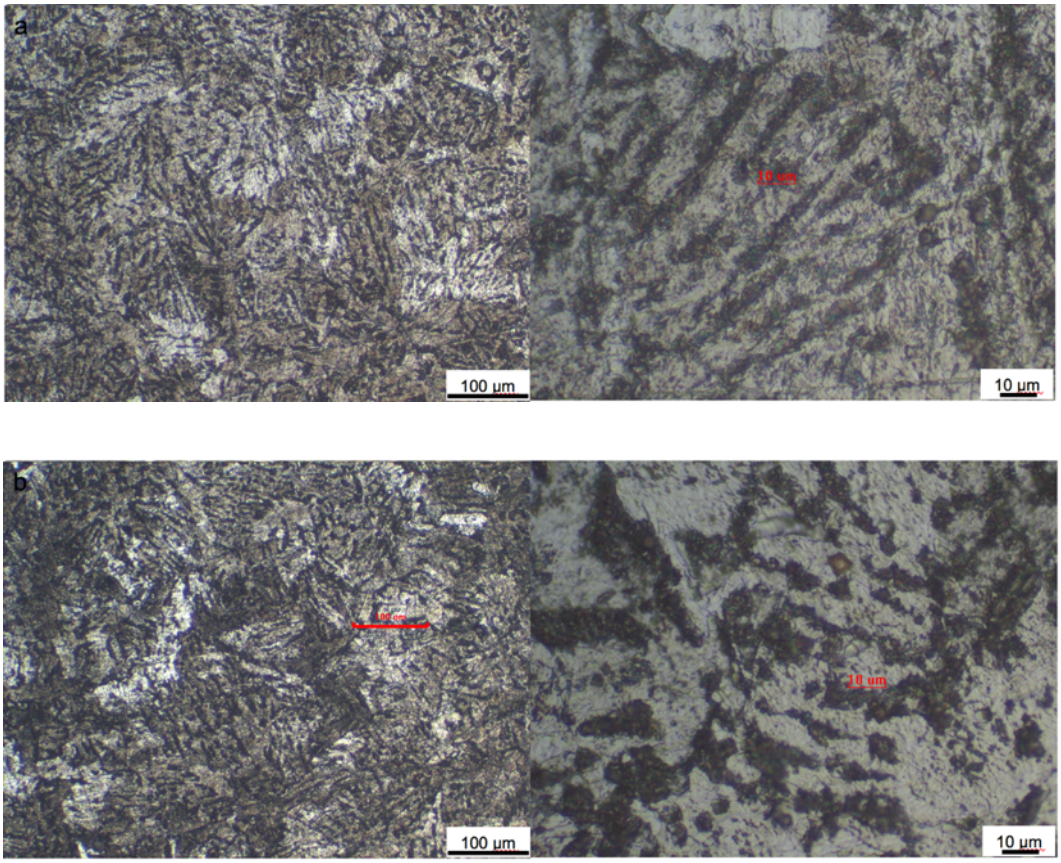

Figure 19. Optical micrograph of samples produced by the aerosol approach, B with different Nb content: a) B1 with 0.1 wt% and b) B2 with 0.5 wt%.

3.3.3 Dispersion of Injected Nanoparticles

First the dispersion and injection efficiency of samples A1, A2, B1 and B2 were evaluated using elemental mapping and EDS spectra. As shown in Figure 20, the EDS spectra for sample A1, using conventional metallurgy with 0.1wt% Nb injection, has no peak for Nb but only peaks for carbon and iron. Coupled with the elemental mapping, which depicted only noise instead of real signal, it indicates that the distribution of Nb powder (micron scale) was very poor when using regular alloying. For sample A2 with

0.5 wt% injection, though the successful introduction of aimed particles was confirmed by those bright red spots which represent the real signal on elemental mapping and the strong peak for Nb in EDS spectra, large aggregation and heterogeneous dispersion of the regular size Nb particles was also clearly revealed. In contrast, as shown in Figure 20a) and and 20b , samples B1 and B2 exhibited much better distribution of the Nb NPs, no aggregation was observed while the strong peaks from EDS spectra also confirmed the effective injection of Nb NPs even with trace amounts as low as 0.1 wt%.

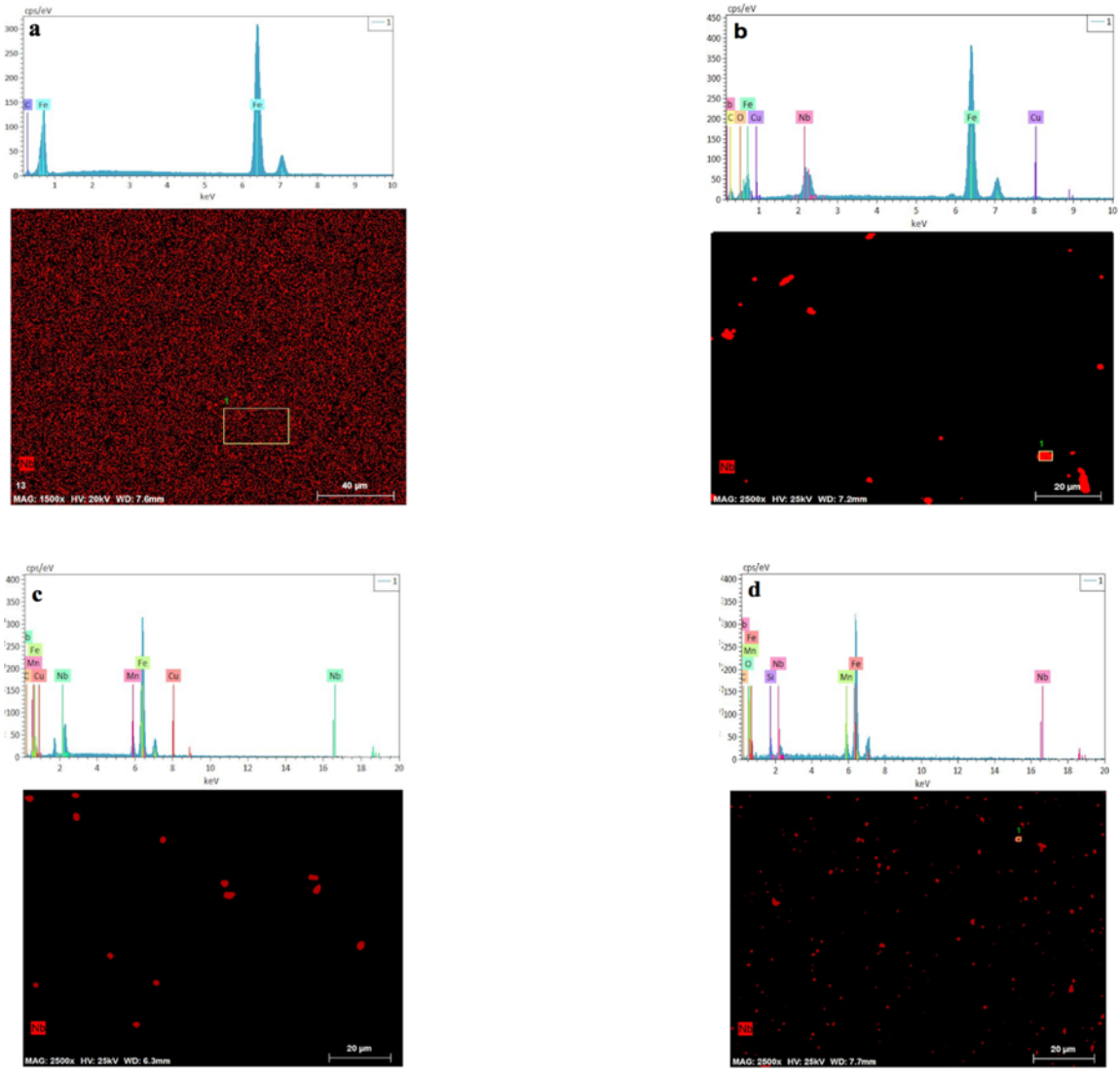

Figure 20. Elemental mapping and EDS spectra for 1018 steel alloy (a) A1, 0.1 wt% Nb powder (< 45 μm) by regular alloying (b) A2, 0.5 wt% Nb powder (< 45 μm) by regular alloying (c) B1,0.1 wt% Nb NPs by aerosolizing and (d) B2, 0.5 wt% Nb NPs by aerosolizing.

Based on the results from SEM and EDS, comparisons were made by setting one parameter constant so as to investigate the importance of the other two parameters (particle size and alloying method). As shown in Figure 21, though samples B2 and D2 both have 0.5 wt% Nb NPs injected, D2, which was prepared by regular alloying, showed poor dispersion and severe aggregation. Even when nanoparticles are used, regular alloying still resulted in heterogeneous dispersion and particle aggregation.

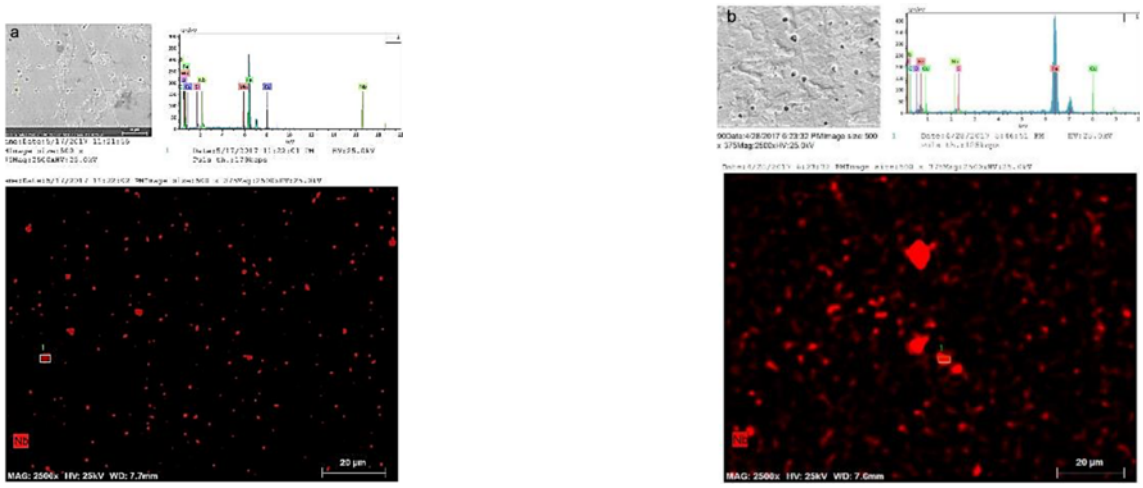

Figure 21. Elemental mapping and EDS spectra for 1018 steel alloy samples (a) B2, 0.5 wt% Nb NPs by aerosolizing (b) D2, 0.5 wt% Nb NPs by regular alloying.

Another comparison between B2 and C2 was made to study the effect of particle size. While sample C2 has relatively good dispersion of Nb particles B2 shows better dispersion over C2.

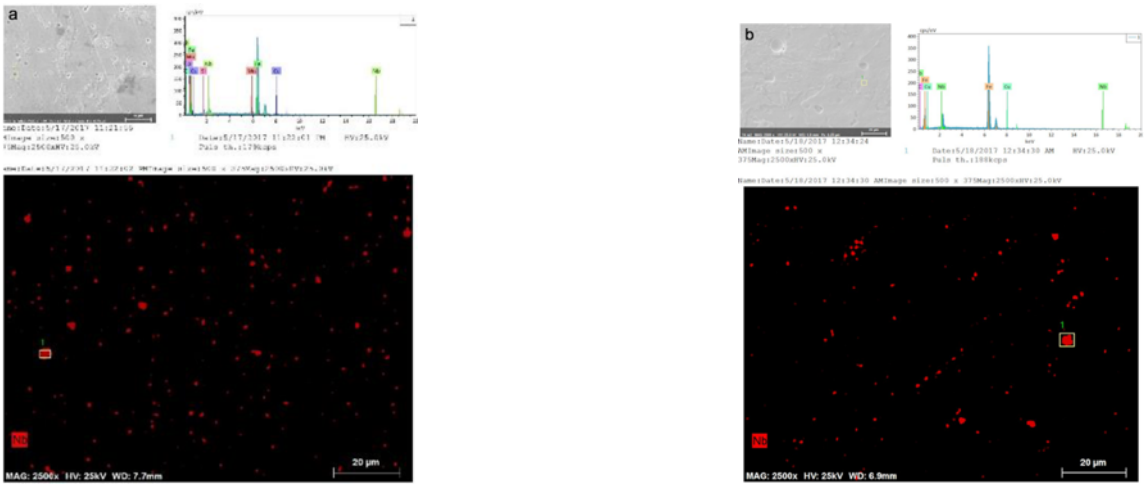

Figure 22. Elemental mapping and EDS spectra for 1018 steel alloy samples (a) B2, 0.5 wt% Nb NPs by aerosolizing (b) C2, 0.5 wt% Nb powder (< 45 µm) by aerosolizing.

Investigation on the effect of aerosolizing was also conducted by comparing samples A2 and C2. With the same amount injection of Nb powder (< 45 µm), sample C2 based on aerosolizing oduction showed much better dispersion than A2 which was prepared by regular alloying. These results suggest that even when the particle size is at micron scale, aerosolizing is still a promising way to have those "large" particles injected and well dispersed into the steel matrix (Figure. 23).

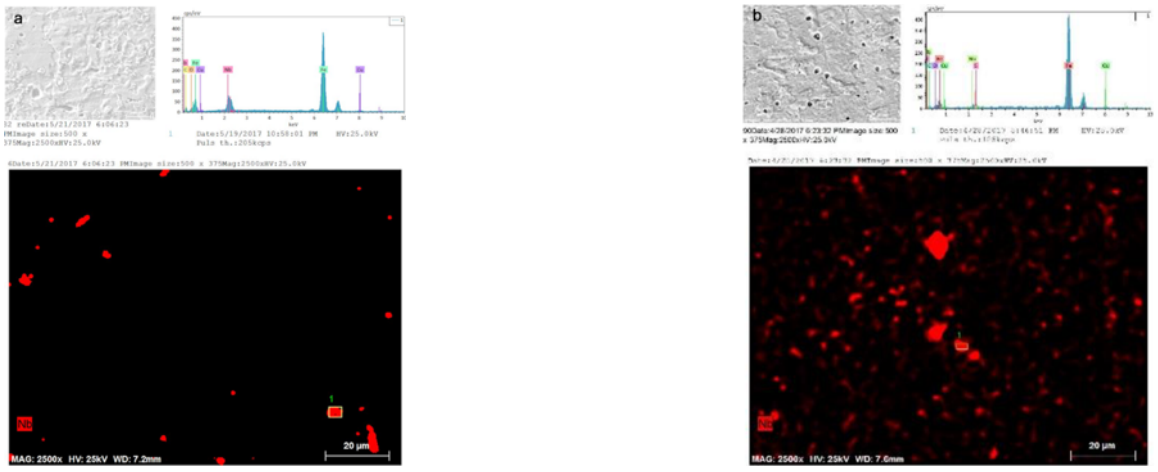

Figure 23. Elemental mapping and EDS spectra for 1018 steel alloy samples (a) A2, 0.5 wt% Nb powder (< 45 µm) by regular alloying (b) C2, 0.5 wt% Nb powder (< 45 µm) by aerosolizing.

The last comparison aimed to confirm the advantage of this novel approach over conventional metallurgy. Sample B2 using Nb NPs and aerosolizing exhibits superior dispersion and no aggregation at all while the sample A2 has severe aggregation and poor distribution (Figure 24).

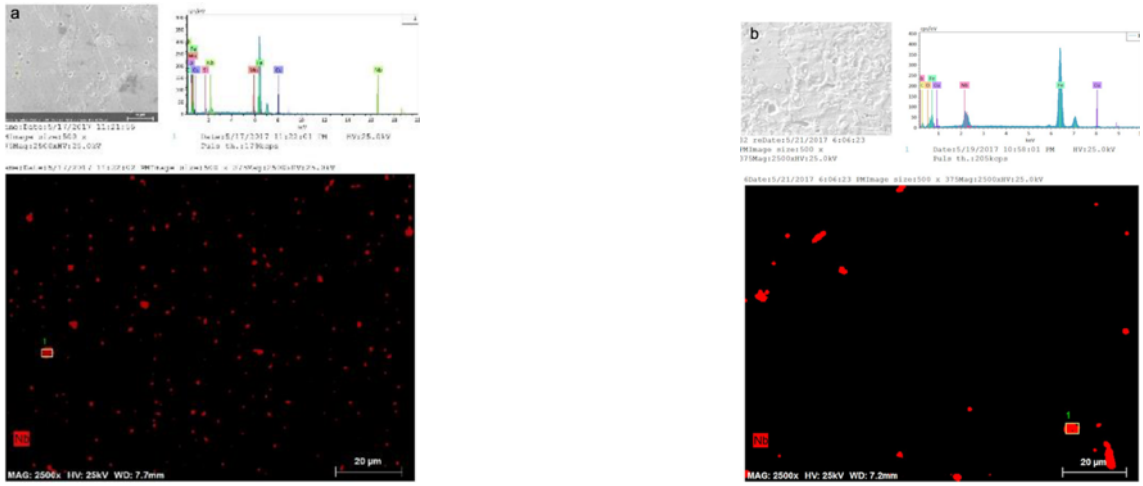

Figure 24. Elemental mapping and EDS spectra for 1018 steel alloy samples (a) B2, 0.5 wt% Nb NPs by aerosolizing (b) A2, 0.5 wt% Nb powder (< 45 μm) by regular alloying.

In fact, among all the samples, B2 using Nanoparticle-Aerosol Technology exhibits the best dispersion of alloyed agents while A2 using conventional metallurgy showed the worst distribution with severe aggregation. Based on these results, at least in aspects of distribution of alloyed agent, Nanoparticle-Aerosol Technology is the most advantageous.

3.3.4 Hardness Tests

The hardness measurement of plain 1018 steel control and other samples based on different processing with different concentrations were performed by using hardness tester, in accordance with Rockwell B standard. The results are summarized in Table 4.

Table 4. Hardness of plain 1018 steel control and samples based on different alloying processing.

	Hardness (Rockwell B)
1018 steel (control)	68.7 ± 1.8
A1 (0.1% Nb < 45um regular alloying)	60.5 ± 1.4
B1 (0.1% Nb NPs aerosolizing)	75.7 ± 2.7

A2 (0.5% Nb < 45um regular alloying)	78.3 ± 1.5
B2 (0.5% Nb NPs aerosolizing)	83.7 ± 1.1
C2 (0.5% Nb < 45um, by aerosolizing)	83.8 ± 0.2
D2 (0.5% Nb NPs, by regular alloying)	74.2 ± 0.6

In general, with increasing amount of Nb 1018 steel alloys show increased hardness. Sample B1, which was prepared by the new approach showed a significant improvement of hardness compared to the control, even with small additions of Nb. Meanwhile, sample A1 produced by conventional metallurgy shows lower hardness than the control. The results are consistent with metallography and EDS mapping in terms of grain size and homogeneity. Samples A2 and C2, both using aerosolizing show about 21% improvement of hardness compared to the control with just 0.5 wt% Nb injected. Comparison (Figure. 23) between A2 and C2 shows that the dispersion of Nb was better in A2 but this advantage is not reflected in the hardness.

3.4 Conclusions

A number of Nb alloys based on 1018 low carbon steel were prepared using different size particles and processing methods. Samples were designed to be prepared with very low content of Nb (0.1 wt% and 0.5 wt%) and macro- or nano-scale particles. Regular alloying versus aerosolizing was examined. Samples prepared by our novel approach

(using nanoparticles and aerosolizing) with even trace amount of injection can still exhibit significantly altered microstructures and mechanical properties. Moreover, samples prepared by Nanoparticle-Aerosol Technology can achieve the most homogeneous dispersion of alloyed agents (even for the particles with micron scale) while the samples made through conventional metallurgy showed the worst dispersion and aggregation of alloyed particles. Based on these results, Aerosol injection shows significant promise as a processing method. When combined with the use of nanoparticles the approach shows the most promise.

REFERENCES

[1] Vural, M., G. Ravichandran, and D. Rittel, *Metallurgical and Materials Transactions A*, **34(12)**:2873-2885 (2003).

[2] Jiang, W. H., and R. Kovacevic, *Proceedings of the Institution of Mechanical Engineers, Part B: Journal of Engineering Manufacture,* **218(10)**:1323-1331(2004).

[3] Xie, Kelvin Y., Tianxiao Zheng, Julie M. Cairney, Harold Kaul, James G. Williams, Frank J. Barbaro, Chris R. Killmore, and Simon P. Ringer, *Scripta Materialia*, **66(9)**:710-713 (2012).

[4] Wenhao Zhou, Hui Guo, Zhenjia Xie, Xuemin Wang, Chengjia Shang, *Pure Appl.Chem*, **587**:365-371 (2013).

[5] S.S. HANSEN, J.B VANDER SANDE and MORRIS COHEN, *METALLURGICAL TRANSACTIONS A*, **11A**: 387-402 (1980).

[6] Girault, Etienne, Pierre Jacques, Ph Harlet, Koen Mols, Jan Van Humbeeck, Etienne Aernoudt, and Francis Delannay, *Materials Characterization*, **40(2)**: 111-118 (1998).